Title

Design of controllers with distributed central pattern generator architecture for adaptive oscillations

Journal

International Journal of Robust and Nonlinear Control, 31(2)

ISSN

1049-8923

Authors

Wu, Andy
Iwasaki, Tetsuya

Publication Date

2021-01-25

DOI

10.1002/rnc.5307

Received: Added at production | Revised: Added at production | Accepted: Added at production

DOI: xxx/xxxx

RESEARCH ARTICLE

Design of controllers with distributed central pattern generator architecture for adaptive oscillations

Andy Wu | Tetsuya Iwasaki

Department of Mechanical and Aerospace Engineering, University of California, Los Angeles, CA, USA

Correspondence
Andy Wu, Department of Mechanical and Aerospace Engineering, University of California, Los Angeles, CA, USA.
Email: anwu@ucla.edu

Present Address
Andy Wu, Department of Mechanical and Aerospace Engineering, University of California, Los Angeles, CA, USA

Funding Information
This research was supported by the National Science Foundation, grants No.1068997 and No.1427313.

Abstract

This paper introduces a systematic method for designing a distributed nonlinear controller to achieve multiple distinct gaits, each of which is characterized by a prescribed oscillation profile and velocity, for a class of locomotion systems. We base the controller on the central pattern generator (CPG), a neural circuit which governs repetitive motions, such as walking and swimming, in most animals. First, we establish a general method for designing a nonlinear CPG-inspired controller to assign a single gait for a linear plant; we show that this problem reduces to an eigenstructure assignment problem for which a solution has recently become available. We then extend the design to an adaptive, structured controller that can adjust the gait in response to variations in the environment. The essential problem becomes a controller design to satisfy different eigenstructure conditions for different plants; a computationally tractable formulation is provided for this problem. We provide two numerical examples using a link-chain model as a plant representative of animals that move through undulatory motions, such as leeches or eels, to demonstrate the efficacy of this theory. In the first example, we employ an analytical condition for eigenstructure assignment to design an unstructured controller that assigns a single gait for the link-chain model. The second example searches for a structured controller to assign two different gaits that can be switched using a higher level command.

KEYWORDS:
Eigenstructure Assignment; Central Pattern Generator; Nonlinear Control; Coordinated Control; Oscillation Control

1 | INTRODUCTION

The analysis and design of feedback controllers for locomotion systems are active fields of research seeking to bridge the gap between biology and robotics. Many of the existing controllers for engineering applications are inspired by the central pattern generator (CPG) [1,2], a biological neural circuit responsible for controlling rhythmic body motions, such as walking, flying, and swimming, in various animals [3,4,5,6,7,8,9]. As a biological circuit, the isolated CPG displays coordinated oscillations that resemble the body movements in terms of the phase pattern and cycle period [10,11,12,13]. While a CPG acts as a reference command generator for muscle contraction, it also modifies and regulates the oscillation pattern through sensory feedback of proprioceptive information [14,15]. These autonomous, coordinated oscillations are realized as orbitally stable limit cycles embedded in the nonlinear dynamics of neuronal circuits interacting with the body biomechanics as well as the environment. It has been observed

that the biological CPG has the capability of generating oscillations that can adapt to different environments[2,8,12,14,15], which would be extremely beneficial for robotic locomotion. Aside from the adaptive limit cycle behavior, CPGs generally have a distributed structure[1,2,14,15], which may provide additional benefits, such as reduction in complexity over centralized controllers[1] and robustness against neuromechanical failures[16]. Due to these features, the dynamical architecture of CPGs provides a viable basis for feedback control design that aims for adaptive oscillations in robotic and other applications.

Many of the CPG-based controllers in bio-inspired robotics have been developed for specific body configurations, including bipeds[17], quadrupeds[18,19,20], hexapods[21], and a hybrid walker/swimmer[22,23]. The network topology of the CPG is typically set *a priori* from the given body configuration in a distributed manner; for instance, a half-center model[24] is placed for each limb with additional coupling for coordination[17]. Such CPG architectures often possess symmetry, which analytically implies possible gaits[25,26] and makes manual parameter tuning tractable with some heuristic design rules[19]. The symmetry and basic building blocks have also been useful in developing models of biological CPGs with overwhelming complexity[27]. In fact, it is possible to design a coupled oscillator network with arbitrary (connected) topology to achieve any desired oscillation pattern with a theoretical guarantee for orbital stability[28,29,30]. However, all these developments (except for[17]) are focused on the design/modeling of the CPG as a reference generator without the plant dynamics (body and environment) in the feedback loop. To exploit the full potential of CPGs for adaptive oscillations, it is essential to design a CPG-based controller with sensory feedback so that a desired oscillation is achieved as a stable limit cycle for the closed-loop system.

A classical, seminal work on the CPG-based feedback control dates back to 1991[17], where coupled half-center oscillators are mutually entrained with a bipedal walker to achieve a stable gait. This approach was used with additional reflex loops and applied to quadruped walking, with experimentally demonstrated potential for adaptivity to irregular terrain[31]. While these results require manual tuning of design parameters, analytical conditions have also been derived for half-center CPGs to entrain to a selected mode of mechanical resonance[32,33]. A more explicit approach to resonance entrainment was proposed using adaptive frequency Hopf oscillators with sensory feedback[34,35], which has been extended with a rigorous proof of stability[36]. Without restrictions to resonance, an arbitrary oscillation pattern can also be achieved with stability for mechanical systems using Hopf oscillators[37,38] or circulant CPGs[39]. However, these methods make the closed-loop system an oscillator through reflex loops and are different from neural control mechanisms where the CPG and plant dynamics are coupled, and hence it is not clear if biological adaptivity can be realized in this way. To date, it still remains open to develop a general theory for designing CPG-inspired controllers that are distributed, can achieve specified body oscillations and velocities under closed-loop with plant dynamics, and have the ability to change gaits to adapt to different environments.

In this paper, we present a solution to the problem of designing a nonlinear feedback controller inspired by the CPG to achieve a specified gait, described by the coordinated oscillations of state variables of a plant to be controlled (e.g. mechanical body subject to environmental dynamics). The design is based on a linear time-invariant model that approximates the plant, but will be effective for the original nonlinear plant dynamics due to structural stability as demonstrated later. We represent the controller as the interconnection of identical neurons with dynamics described by a threshold nonlinearity in series with a first-order low pass filter. In our analysis, the threshold nonlinearity is quasi-linearized using a describing function and the governing equations are developed using the multivariable harmonic balance (MHB) method[40]. The problem is then reduced to the design of a quasi-linear controller such that the closed-loop system is marginally stable with the pair of conjugate eigenvalues representing the frequency of the desired oscillation and corresponding eigenvectors specified by the desired phase and amplitude. The design can then be performed using an existing solution to the eigenstructure assignment problem in[41].

As an extension to the single gait design, we further consider the design of a single structured CPG-inspired controller that can adapt its gait to its environment. This problem is conceived as an eigenstructure assignment in which a single controller, parameterized by an adaptation parameter τ, is designed to assign multiple eigenstructures to multiple plants, depending on the value of τ. In a typical application scenario, each of the multiple plants is composed of the same robotic locomotion system with different environmental dynamics. In this case, the controller will be able to achieve gait transition by adjusting τ in accordance with the changing environment. We will reduce the control design to a cone complementarity problem — minimization of $\mathrm{tr}(PR)$ subject to linear matrix inequality constraints on symmetric matrices P and R. The problem is nonconvex and is difficult to solve with a theoretical guarantee for global optimality. However, there are computational algorithms that are applicable to this class of problems with practical reliability[42,43,44]; the linearization algorithm[43] in particular will be shown to be effective for our design.

The proposed design methods are based on a linear plant with harmonic approximations and do not rigorously guarantee convergence to the target limit cycle oscillations. However, we demonstrate the efficacy of the design methods with two examples utilizing a nonlinear link-chain model for undulatory swimming provided by[45,46] and experimentally observed leech gaits from[15].

In the first example, we design an unstructured controller to achieve a gait mimicking that of a leech in water. In the second example, we design a single structured controller parameterized by neural time constant τ to achieve the observed leech gaits for fast and slow swimming in two different fluid environments (water and high viscosity methyl cellulose). The adjustment of the parameter τ empirically captures the descending drive from the brainstem to the CPG that regulates the frequency of oscillation[47,27]. This type of mechanism has been used for gait transition in the open-loop setting[23]. We will propose a simple adaptation mechanism to adjust τ based on the swim speed v in real time, and further demonstrate the ability to autonomously switch gaits when the fluid environment changes.

Preliminary versions of this paper have been presented at conferences[48] and[49], where some basic ideas for the CPG-based control design are laid out. The present paper formalizes the ideas and provides systematic design procedures, with a major extension to allow for embedding multiple stable limit cycles using a distributed CPG architecture. The design examples are completely new.

Notation: Let $\mathbb{R}$ and $\mathbb{I}_n$ denote the sets of real numbers and integers $\{1, \dots, n\}$, respectively. For a matrix M, the notations $M^\intercal$ and $M^\dagger$ denote the transpose and the Moore-Penrose inverse, respectively. The symbol $\mathrm{diag}(A_1, \dots, A_n)$ denotes the block-diagonal matrix with $A_1, \dots, A_n$ on the diagonal, and $\mathrm{col}(B_1, \dots, B_n)$ denotes the matrix obtained by stacking $B_1, \dots, B_n$ in a column. The real and imaginary parts of a vector are denoted by $\mathfrak{R}(\cdot)$ and $\mathfrak{I}(\cdot)$, respectively.

2 | PROBLEM FORMULATION AND APPROACH

2.1 | Problem Statement

Let a linear time-invariant plant be given by a state-space realization

$$\dot{x} = Ax + Bu, \quad y = Cx \tag{1}$$

where $x(t) \in \mathbb{R}^n$ is the state, $u(t) \in \mathbb{R}^m$ is the control input, and $y(t) \in \mathbb{R}^p$ is the measured output. Throughout the paper, we assume that (A, B, C) is stabilizable and detectable. The problem of designing a controller to achieve oscillations can be described as follows.

Problem 1. Let a desired oscillation profile be defined by the frequency ω, amplitude a_i, and phase b_i for $i \in \mathbb{I}_n$. Suppose $\omega > 0$ and at least one of parameters a_i is nonzero. Given a linear plant (1), find a nonlinear dynamic output-feedback controller such that the closed-loop system has an orbitally stable limit cycle on which $x_i(t) \cong a_i \sin(\omega t + b_i)$ holds approximately for all $i \in \mathbb{I}_n$.

Orbital stability is a property of a periodic solution of the closed-loop system. In particular, let $q(t)$ be the controller state vector and denote the closed-loop state by $\mathrm{x} := \mathrm{col}(x, q)$. A periodic solution $\mathrm{x}(t)$ is said to be orbitally stable if all trajectories converge to the periodic orbit

$$\mathbb{O} := \{\, x(t) \in \mathbb{R}^n \,:\, t \in \mathbb{R} \,\},$$

whenever the initial conditions $\mathrm{x}(0)$ are sufficiently close to the orbit[50].

Due to the linearity of the plant, a nonlinear controller is necessary for orbital stability as linear oscillations lack the structural stability to reject perturbations to their trajectories. For the controller, we choose one with the CPG control architecture because the CPG is a well-studied nonlinear oscillator that generates stable limit cycles when placed in a feedback loop with the body-environment dynamics[51,52,53,54,55,15]. We will fix the architecture of the controller and reformulate the problem such that we can search for the design parameters in a numerically tractable manner.

2.2 | CPG Control Architecture

The CPG is a biological neuronal circuit existing in various animals that commands rhythmic muscle contractions which result in repetitive motions such as walking, breathing, or chewing. When isolated, the CPG is a nonlinear oscillator that has a profile similar to observed body motions. This oscillation results in a stable limit cycle that corresponds to a gait or repetitive movement when placed in a closed loop with the body-environment dynamics.

Mathematically, the CPG is often expressed as a system of interconnected neurons which are individually defined as a static nonlinearity in series with a linear filter. In the case of a set of n_c interconnected neurons, the CPG can be given by the scalar

equations

$$v_i = \psi(q_i), \quad q_i = f(s)w_i, \quad w_i = \sum_{j=1}^{n_c} \mu_{ij} v_j$$

for $i \in \mathbb{I}_{n_c}$, where ψ is a static nonlinearity which emulates the neural threshold property observed in biology[47], $f(s)$ is a linear filter that captures the dynamical properties of neuronal cell membranes such as adaptation or time lag, μ_{ij} defines the synaptic connection strength and type (excitatory or inhibitory) from neuron j to neuron i, and w_i, q_i, and v_i represent the input from presynaptic neurons, the cell membrane potential, and instantaneous spike frequency, respectively. Within the scope of this paper, we define ψ and $f(s)$ to be

$$\psi(x) = \tanh(x), \quad f(s) = \frac{1}{1+\tau s},$$

with each neuron having identical dynamics, $f(s)$, defined by a neuronal information processing time constant τ. It should be noted that ψ and $f(s)$ are not limited to the choices given above and alternative options exist. The equations defining the set of n_c neurons can be organized in more compact manner by stacking them in matrices:

$$q = F(s)M\Psi(q), \quad v = \Psi(q), \quad w = Mv$$

where $v(t)$, $q(t)$, and $w(t)$ are vectors of dimension n_c, M is the neuronal interconnectivity matrix with μ_{ij} as its $(i,j)^{\text{th}}$ entry, and

$$F(s) := f(s)I_{n_c}, \quad \Psi(q) := \text{col}\Big(\psi(q_1), \ldots, \psi(q_{n_c})\Big).$$

Extending the CPG model to be used as a controller, we feed back measurements from a plant and further define a control output from the CPG controller. In particular, we define the CPG controller as

$$q = F(s)(M\Psi(q) + Hy), \quad u = G\Psi(q) + Ly, \tag{2}$$

where L, G, and H are constant matrices[15]. The sensory feedback signal y from the plant would typically be proprioceptive information (e.g. joint angles) for biological CPGs, but it could be any sensor signals in our theoretical framework for the control design. Figure 1 expresses the closed-loop system in terms of a block diagram, where the blue blocks represent parameters for the CPG controller (2), and $P(s)$ is the plant transfer function from u to y defined by (1). The closed-loop system of (1) and (2) can be given as

$$\begin{bmatrix} \dot{x} \\ \dot{q} \end{bmatrix} = \begin{bmatrix} A & 0 \\ 0 & A_f \end{bmatrix} \begin{bmatrix} x \\ q \end{bmatrix} + \begin{bmatrix} B & 0 \\ 0 & B_f \end{bmatrix} \begin{bmatrix} L & G \\ H & M \end{bmatrix} \begin{bmatrix} C & 0 \\ 0 & I \end{bmatrix} \begin{bmatrix} x \\ \Psi(q) \end{bmatrix} \tag{3}$$

where $A_f := -I/\tau$ and $B_f := I/\tau$ give a minimal state space realization (A_f, B_f, I) of $F(s)$ with state vector q.

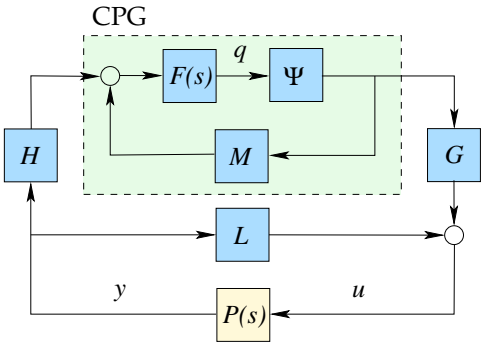

FIGURE 1 Closed-Loop System of CPG and Plant

The oscillation control problem can now be defined as a search for parameters L, G, H, M, and τ to satisfy the specifications from Problem 1. Due to the inherent difficulties of solving nonlinear oscillation problems with guaranteed orbital stability, we will approximate Problem 1 by a more tractable problem through the use of the MHB equation[40].

2.3 | The Multivariable Harmonic Balance

This section describes an approximate condition for a generic system

$$\dot{x} = Ax + Bv, \quad q = Cx, \quad v = \Psi(q), \tag{4}$$

to have a stable limit cycle that can be approximated as

$$x_i(t) \cong \gamma_i \sin(\omega t + \delta_i). \tag{5}$$

The result will be useful for the CPG control design since the closed-loop system in Fig. 1 is a Luré system, i.e. a nonlinear system comprising a linear time-invariant system with a static nonlinearity, and hence (3) can be described in the form (4) with appropriately defined matrices A, B, and C, where the closed-loop state is given by $x := \mathrm{col}(x, q)$.

To facilitate the analysis of oscillations in (4), we reduce the nonlinear system to a quasi-linear form by approximating the static nonlinearity with

$$\psi(q_i) \cong \kappa(\alpha_i) q_i \quad \text{for} \quad q_i = \alpha_i \sin(\omega t),$$

where $\kappa(\alpha_i)$ is the describing function defined such that $\kappa(\alpha_i)q_i$ is equal to the first harmonic of $\psi(q_i)$. Substituting the approximation

$$\Psi(q) \cong \Delta(\alpha) q, \quad \Delta(\alpha) := \mathrm{diag}(\kappa(\alpha_1), \dots, \kappa(\alpha_{n_c})), \quad \alpha := \mathrm{col}(\alpha_1, \dots, \alpha_{n_c})$$

into (4), we have the following quasi-linearized system

$$\dot{x} = \mathfrak{A}x, \quad \mathfrak{A} := A + B\Delta(\alpha)C. \tag{6}$$

Now, the harmonic oscillation in (5) can be described by $\mathfrak{I}[\hat{x}e^{j\omega t}]$, where $\hat{x}$ is the phasor vector specified by $\hat{x}_i := \gamma_i e^{j\delta_i}$. From the standard linear theory, $x(t) = \mathfrak{I}[\hat{x}e^{j\omega t}]$ is an exact solution of the quasi-linear system (6) if and only if the MHB equation

$$(j\omega I - \mathfrak{A})\hat{x} = 0, \quad \hat{x}_i := \gamma_i e^{j\delta_i},$$

holds, where the phasor $\hat{x}$ specifies the amplitude parameter α by

$$\alpha_i = |\hat{q}_i|, \quad \hat{q} := C\hat{x}.$$

The harmonic balance analysis anticipates that the nonlinear system (4) has a periodic solution that is approximately given by (5) if the MHB equation is satisfied. Moreover, the periodic solution is expected to be orbitally stable if the quasi-linear system (6) is marginally stable with a conjugate pair of eigenvalues $\pm j\omega$ on the imaginary axis and the rest in the open left-half plane.

Note that the MHB equation takes the form of eigenvalue and eigenvector relationship with the eigenvalue, $j\omega$, specifying the frequency of oscillation and the eigenvector, $\hat{x}$, specifying the phases and amplitudes. The general idea of the quasi-linearization and the MHB condition described here will be the basis for the control design in the next section.

3 | CPG CONTROL DESIGN

3.1 | Reduction to Eigenstructure Assignment

To obtain a tractable formulation for Problem 1, we will quasi-linearize the closed-loop system in (3) and derive the design equations using the harmonic balance approach in the previous section. The process turns out to give an eigenstructure assignment problem.

On the target limit cycle of the closed-loop system, the controller state $q(t)$ shares the same period as the plant state $x(t)$ and oscillates with frequency ω. We approximate this oscillation by

$$q_i(t) \cong \alpha_i \sin(\omega t + \beta_i)$$

with some amplitude α_i and phase β_i; let the phasor of q_i be given by $\hat{q}_i = \alpha_i e^{j\beta_i}$. Substituting the describing function, $\Delta(\alpha)q$, in place of $\Psi(q)$, the closed-loop system (3) can be quasi-linearized as

$$\dot{x} = \mathfrak{A}x, \quad \mathfrak{A} := \mathcal{A} + \mathcal{B}\mathcal{K}\mathcal{C}, \tag{7}$$

where

$$\mathrm{x} := \begin{bmatrix} x \\ q \end{bmatrix}, \quad \begin{array}{l} \mathcal{A} := \mathrm{diag}(A, 0), \\ \mathcal{B} := \mathrm{diag}(B, I), \\ \mathcal{C} := \mathrm{diag}(C, I), \end{array} \tag{8}$$

$$\mathcal{K} := \begin{bmatrix} 0 & 0 \\ 0 & A_f \end{bmatrix} + \begin{bmatrix} I & 0 \\ 0 & B_f \end{bmatrix} \begin{bmatrix} L & G\Delta(\alpha) \\ H & M\Delta(\alpha) \end{bmatrix}. \tag{9}$$

Note that the system (7) can be seen as the closed-loop system comprised of (1) and dynamic controller

$$\begin{bmatrix} u \\ \dot{q} \end{bmatrix} = \mathcal{K} \begin{bmatrix} y \\ q \end{bmatrix}. \tag{10}$$

Applying the MHB method to (7), the nonlinear closed-loop system, (3), is predicted to have a limit cycle with an oscillation profile, $x_i(t) \cong a_i \sin(\omega t + b_i)$, if there exists a complex vector $\hat{q} \in \mathbb{C}^{n_c}$ such that

$$(j\omega I - \mathfrak{A})\hat{\mathrm{x}} = 0, \quad \hat{\mathrm{x}} := \mathrm{col}(\hat{x}, \hat{q}), \tag{11}$$

hold for $\hat{x}_i = a_i e^{jb_i}$, $i \in \mathbb{I}_{n_c}$, where matrix $\mathfrak{A}$ is defined by (7) and (9) with $\alpha_i := |\hat{q}_i|$. Moreover, the limit cycle is expected to be orbitally stable if all the eigenvalues of $\mathfrak{A}$ other than $\pm j\omega$ are in the open left-half plane. Defining

$$\Lambda := \begin{bmatrix} 0 & \omega \\ -\omega & 0 \end{bmatrix}, \quad \begin{array}{l} X := \begin{bmatrix} \mathfrak{R}(\hat{x}) & \mathfrak{I}(\hat{x}) \end{bmatrix}, \\ Q := \begin{bmatrix} \mathfrak{R}(\hat{q}) & \mathfrak{I}(\hat{q}) \end{bmatrix}, \end{array} \tag{12}$$

the MHB equation (11) can be expressed in terms of real matrices as

$$\mathfrak{A}\mathcal{V} = \mathcal{V}\Lambda, \quad \mathcal{V} := \mathrm{col}(X, Q). \tag{13}$$

Thus the design problem is reduced to the search for real matrices (M, G, H, L) and Q satisfying (13) and the eigenvalue (marginal stability) condition. Note that (9) defines a change of variables $(M, G, H, L) \leftrightarrow \mathcal{K}$, where the mapping is invertible because B_f and $\Delta(\alpha)$ are square invertible. Hence, the essential problem is to find $\mathcal{K}$ and Q satisfying (13) and the marginal stability requirement. Once $\mathcal{K}$ and Q are found, the CPG parameters (M, G, H, L) can be calculated by solving (9) with $\alpha_i := |\hat{q}_i|$. This leads to the following eigenstructure assignment problem.

Problem 2. Consider the plant in (1) and let a desired eigenstructure be specified by $X \in \mathbb{R}^{n\times 2}$ and $\Lambda \in \mathbb{R}^{2\times 2}$, where Λ is of the form in (12) with $\omega \neq 0$, and (X, Λ) is observable. Find a controller $\mathcal{K}$ (of an arbitrary order n_c) in (10) and matrix $Q \in \mathbb{R}^{n_c\times 2}$ such that the closed-loop system in (7) with (8) satisfies (13), matrix $\mathcal{V}$ has rank two, and the eigenvalues of $\mathfrak{A}$ are all in the open left half complex plane except for those shared by Λ.

The rank constraint on $\mathcal{V}$ is imposed because otherwise $\hat{\mathrm{x}} := \mathrm{col}(\hat{x}, \hat{q})$ is a scalar multiple of a real vector, and (11) would then imply $\hat{\mathrm{x}} = 0$, which cannot be the case whenever the desired oscillation is nontrivial. Note that X may not have full column rank in such cases as synchronization $x_i(t) = x_j(t)$ for $i, j \in \mathbb{I}_n$. A factor that makes the problem difficult is the dependence of (13) on the unknown design parameter Q. It turns out, however, that Q can be set, without loss of generality, to an arbitrary matrix with full column rank.

Lemma 1. *Consider Problem 2 and suppose it is feasible. Let $Q \in \mathbb{R}^{n_c\times 2}$ be an arbitrary matrix such that it is of full column rank and $n_c \geq n + 2$. Then there exists a controller $\mathcal{K}$ such that $(\mathcal{K}, Q)$ is a solution to Problem 2.*

Proof. Suppose Problem 2 admits a solution and let Q be given as above. From Theorem 3 of[41], a dynamic controller $\mathcal{K}_o$ of order $n_c \geq n + 2$ solves Problem 2 with $Q_o := \mathrm{col}(I, 0) \in \mathbb{R}^{n_c\times 2}$. Let T_c be a square nonsingular matrix such that $Q = T_c Q_o$. Such T_c exists since Q and Q_o are full column rank. Define

$$\begin{array}{ll} T := \mathrm{diag}(I, T_c), & \mathcal{K} := T\mathcal{K}_o T^{-1}, \\ \mathcal{V}_o := \mathrm{col}(X, Q_o), & \mathfrak{A}_o := \mathcal{A} + \mathcal{B}\mathcal{K}_o\mathcal{C}, \end{array}$$

Then direct calculations verify that

$$\mathfrak{A} = T\mathfrak{A}_o T^{-1}, \quad \mathfrak{A}\mathcal{V} - \mathcal{V}\Lambda = T(\mathfrak{A}_o\mathcal{V}_o - \mathcal{V}_o\Lambda) = 0.$$

Thus we conclude the result. □

Based on Lemma 1, we can set Q to be an arbitrary full column-rank matrix when solving Problem 2. Equivalently, $\hat{q}$, the phasor of the CPG variable $q(t)$, is set to an arbitrary complex vector that is not a scalar multiple of a real vector. This means that at least one pair of the CPG variables $q_i(t)$ should oscillate with relative phase not equal to zero or π. The choice of $\hat{q}$ does not matter in Problem 2 because it just corresponds to the coordinate change in the controller state. However, the choice is important and affects the oscillation property of the nonlinear closed-loop system. In particular, when the amplitude $\alpha := |\hat{q}|$ is large, the nonlinearity $\Psi(q)$ tends to saturate, making the approximation by the describing function $\Psi(q) \cong \Delta(\alpha)q$ less accurate. On the other hand, the nonlinear effect is crucial for achieving orbital stability of the target limit cycle.

We propose to set $\hat{q}$ using the concept of coupled segmental oscillators found in neuronal CPG circuits[56,47]. Adopting this control architecture (a specific example will be given later in Fig. 2), each actuator is driven by a segmental oscillator — a set of neurons that oscillate together with specific phase differences, and the controller is formed as coupled m segmental oscillators where m is the number of control inputs. For example, each segmental oscillator may be formed by ℓ neurons that oscillate with the same amplitude with phases evenly distributed over 2π. The relative phases between segments may be set to match those between actuation signals $u(t) \in \mathbb{R}^m$ that generate the desired oscillations for $x(t) \in \mathbb{R}^n$. In this case, $\hat{q} \in \mathbb{C}^{n_c}$ is set to

$$\begin{aligned} &\hat{q} := \mathrm{col}(\hat{p}_1, \dots, \hat{p}_m), \quad \hat{p}_i := \gamma r e^{j\theta_i}, \\ &r := \mathrm{col}(e^{j\varphi}, e^{j2\varphi}, \dots, e^{j\ell\varphi}), \quad \varphi := 2\pi/\ell, \\ &\hat{u} := B^\dagger(j\omega I - A)\hat{x}, \quad \theta_i := \angle \hat{u}_i, \end{aligned} \tag{14}$$

where the total number of neurons is $n_c := m\ell$, and $\gamma \in \mathbb{R}$ is the uniform amplitude of $q_i(t)$ for all $i \in \mathbb{I}_{n_c}$.

The next section will describe a systematic method for solving Problem 2. The section that follows will address the structured control design. In particular, Problem 2 is solved directly for the CPG parameter (M, G, H, L) instead of $\mathcal{K}$ with an additional structural constraint on the design parameter. The whole design process will then be summarized.

3.2 | General Unstructured Control Design

This section considers Problem 2 with no constraints on the controller structure. In this case, a complete solution for the eigenstructure assignment is given in[41]. The essential result summarized below will be useful for checking feasibility of the desired oscillation and for developing a baseline design before proceeding to the design of a distributed controller to achieve multiple oscillations as described in the next section.

Theorem 1. [41] *The following statements are equivalent.*

(i) Problem 2 admits a solution $(\mathcal{K}, Q)$.

(ii) There exists a matrix U *such that*

$$AX + BU = X\Lambda. \tag{15}$$

In this case, the controller[1]

$$\begin{bmatrix} u \\ \dot{\zeta} \end{bmatrix} = \begin{bmatrix} U \\ \Lambda \end{bmatrix} \zeta + \mathcal{S}(s)(y - CX\zeta). \tag{16}$$

solves Problem 2 with $Q = col(I, 0)$*, where* $\mathcal{S}(s)$ *represents an arbitrary linear time invariant system that internally stabilizes the augmented plant* $C(sI - A)^{-1}\mathfrak{B}$ *with* $\mathfrak{B} := \begin{bmatrix} B & -X \end{bmatrix}$.

Condition (15) is called the regulator equation and its solvability for U is necessary and sufficient for the existence of $u(t)$ that makes $x(t)$ oscillate as $x(t) = \mathfrak{R}[\hat{x}e^{j\omega t}]$. The regulator equation is linear and can readily be solved for U whenever a solution exists. The control input is then given by $u(t) = \mathfrak{R}[\hat{u}e^{j\omega t}]$ with $\hat{u} := U\mathrm{col}(1, j)$. In fact, an explicit formula for $\hat{u}$ can be given as in (14).

A state space realization of the controller in (16) gives a solution to Problem 2 as

$$\begin{bmatrix} u \\ \dot{q}_o \end{bmatrix} = \mathcal{K}_o \begin{bmatrix} y \\ q_o \end{bmatrix}, \quad q_o := \begin{bmatrix} \zeta \\ x_s \end{bmatrix}$$

[1] The notation such as $\mathcal{S}(s)y$ in a time-domain equation means the inverse Laplace transform of $\mathcal{S}(s)Y(s)$ where $Y(s)$ is the Laplace transform of $y(t)$.

where

$$\mathcal{K}_o := \left[\begin{array}{c|cc} D_{s1} & U - D_{s1}CX & C_{s1} \\ \hline D_{s2} & \Lambda - D_{s2}CX & C_{s2} \\ B_s & -B_sCX & A_s \end{array}\right], \tag{17}$$

with the partitions in accordance with the dimensions of (u, y, q_o), and

$$\mathcal{S}(s) := \begin{bmatrix} C_{s1} \\ C_{s2} \end{bmatrix} (sI - A_s)^{-1} B_s + \begin{bmatrix} D_{s1} \\ D_{s2} \end{bmatrix}$$

is the transfer function of a controller with state vector x_s that stabilizes the augmented plant $(A, \mathfrak{B}, C)$. The controller $\mathcal{K}_o$ achieves the desired oscillation of $x(t)$ for the linear closed-loop system (7) with the particular eigenmatrix $Q_o = \mathrm{col}(I, 0)$. This means that the state $q_o(t)$ of the controller $\mathcal{K}_o$ converges as

$$\zeta(t) \to \begin{bmatrix} r\sin(\omega t + \rho) \\ r\cos(\omega t + \rho) \end{bmatrix}, \quad x_s(t) \to 0$$

in the steady state, where (r, ρ) are parameters that depend on the initial state x(0). The speed of convergence is dictated by the eigenvalues of the closed-loop system of the augmented plant $(A, \mathfrak{B}, C)$ and the stabilizing controller $\mathcal{S}(s)$.

Given a phasor $\hat{q} \in \mathbb{C}^{n_c}$ for the target oscillation of the controller state $q(t)$ with an arbitrary dimension $n_c \geq 2$, the eigenmatrix Q is set by (12), and the controller $\mathcal{K}$ that assigns the eigenstructure $\mathrm{col}(X, Q)$ and solves Problem 2 with the given Q is obtained as follows. First, design a controller $\mathcal{K}_o$ of order n_c that assigns $\mathrm{col}(X, Q_o)$, using a stabilizing controller $\mathcal{S}(s)$ of order $n_c - 2$ as in Theorem 1. This step requires $n_c \geq 2$, and is easily done if $n_c \geq n + 2$ using an observer-based controller $\mathcal{S}(s)$. The eigenmatrix Q_o for the controller state can be transformed into any other full column-rank matrix of the same dimensions through a similarity transformation on the controller. Thus the next step is to obtain $\mathcal{K}$ from $\mathcal{K}_o$ through a state coordinate transformation $q = T_c q_o$. In particular, the similarity transformation matrix takes the form $T_c = [Q\ N]$, where N is an arbitrary matrix that makes T_c square invertible. The transformed controller is then given as $\mathcal{K} = T\mathcal{K}_o T^{-1}$ with $T := \mathrm{diag}(I, T_c)$.

3.3 | Structured Control for Multiple Eigenstructures

In this section, we consider Problem 2 with a constraint on the controller structure. Specifically, controller matrix $\mathcal{K}$ sought in Problem 2 is seen as a linear function (9) of the parameter $\sigma := (M, G, H, L)$ which is required to lie in a given set $\mathbb{S}$. In our formulation described below, the set $\mathbb{S}$ can be an arbitrary finite dimensional convex set, but of particular interest is the case where certain entries of matrices (M, G, H, L) are constrained to be zero, which is useful for distributed CPG design. Our method naturally extends to the design of a single structured controller to assign multiple eigenstructures to multiple plants. Such design is relevant for construction of an adaptive CPG controller to achieve multiple gaits under varying environment. These applications will be illustrated later by design examples.

The eigenstructure assignment in Problem 2 requires that the spectrum of the closed-loop system matrix $\mathfrak{A}$ contains the eigenvalues of Λ and all the remaining eigenvalues of $\mathfrak{A}$ have negative real parts. We will first isolate the eigenspaces associated with these two groups of the eigenvalues. Let $(\mathcal{N}, \mathcal{U}, \mathcal{W})$ be any matrix triple determined from $\mathcal{V}$ such that

$$\begin{bmatrix} \mathcal{U}^\intercal \\ \mathcal{W}^\intercal \end{bmatrix} \begin{bmatrix} \mathcal{V}\ \mathcal{N} \end{bmatrix} = \begin{bmatrix} \mathcal{V}\ \mathcal{N} \end{bmatrix} \begin{bmatrix} \mathcal{U}^\intercal \\ \mathcal{W}^\intercal \end{bmatrix} = I. \tag{18}$$

Then, by a similarity transformation, we have

$$\begin{bmatrix} \mathcal{U}^\intercal \\ \mathcal{W}^\intercal \end{bmatrix} \mathfrak{A} \begin{bmatrix} \mathcal{V}\ \mathcal{N} \end{bmatrix} = \begin{bmatrix} \Lambda & \mathcal{U}^\intercal \mathfrak{A} \mathcal{N} \\ 0 & \mathcal{W}^\intercal \mathfrak{A} \mathcal{N} \end{bmatrix} \tag{19}$$

where condition (13) is used. Hence, the eigenvalue requirement on $\mathfrak{A}$ is satisfied when $\mathcal{W}^\intercal \mathfrak{A} \mathcal{N}$ is Hurwitz. The basic problem then is to find $\sigma \in \mathbb{S}$ such that $\mathcal{W}^\intercal \mathfrak{A}(\sigma) \mathcal{N}$ is Hurwitz and (13) is satisfied, where the dependence of $\mathfrak{A}$ on σ is made explicit. With given X and Q, constraint (13) is linear in σ and defines a convex set of parameters σ (denote this set by $\mathbb{E}$). Therefore, the problem is a special case of the following general structured stabilization problem with variable σ, feasible domain $\mathbb{F} := \mathbb{S} \cap \mathbb{E}$, and characteristic matrix $\mathcal{A}(\sigma) := \mathcal{W}\mathfrak{A}(\sigma)\mathcal{N}$.

Problem 3. Let $\mathbb{F}$ be a finite dimensional convex set, and $\mathcal{A}(\sigma)$ be a square-matrix function that depends affinely on $\sigma \in \mathbb{F}$. Find a parameter $\sigma \in \mathbb{F}$ such that matrix $\mathcal{A}(\sigma)$ has eigenvalues in the open left half plane.

The structured stabilization problem is known to be extremely difficult, and we will suggest a heuristic solution method here and demonstrate its utility by a design example later. Recall that all the eigenvalues of $\mathcal{A}(\sigma)$ have negative real parts if and only if there exist a (sufficiently small) scalar $\varepsilon > 0$ and symmetric matrix P such that

$$(I + \varepsilon\mathcal{A}(\sigma))^{\mathsf{T}} P (I + \varepsilon\mathcal{A}(\sigma)) < P, \quad P = P^{\mathsf{T}} > 0. \tag{20}$$

This condition is actually necessary and sufficient for the eigenvalues of $\mathcal{A}(\sigma)$ to be inside the circle of radius $1/\varepsilon$ with center at $-1/\varepsilon$, and easily follows from standard results on eigenvalue characterizations (e.g.[57]). Using the Schur complement and the idea in[43], it can be verified that the search for σ and P satisfying (20) with a fixed small $\varepsilon > 0$ can be reduced to

$$\min_{P,R,\sigma\in\mathbb{F}} \ \mathrm{tr}(PR) \tag{21}$$

subject to

$$\begin{bmatrix} P & I \\ I & R \end{bmatrix} \geq 0, \quad \begin{bmatrix} P & I + \varepsilon\mathcal{A}(\sigma)^{\mathsf{T}} \\ I + \varepsilon\mathcal{A}(\sigma) & R \end{bmatrix} > 0. \tag{22}$$

In particular, (20) is feasible for P and $\sigma \in \mathbb{F}$ if and only if the minimum of this optimization problem is attained at $P = R^{-1}$. The constraints are convex, but the objective function is nonconvex, which makes the problem difficult. However, the linearization algorithm in[43] has been proven, through numerical experiments, to work well in practice for solving this class of optimization problems.

The above formulation trivially extends to Problem 3 with the simultaneous stabilization setting. Suppose we seek a single parameter $\sigma \in \mathbb{F}$ such that $\mathcal{A}_k(\sigma)$ are Hurwitz for $k \in \mathbb{I}_h$, where h is an arbitrary positive integer. Then the optimization problem can be modified so that the variables are σ, P_k and R_k for $k \in \mathbb{I}_h$, the objective function is the sum of $\mathrm{tr}(P_k R_k)$ over $k \in \mathbb{I}_h$, and constraints (22) are repeated h times by replacing P, R, and $\mathcal{A}(\sigma)$ with P_k, R_k, and $\mathcal{A}_k(\sigma)$ for $k \in \mathbb{I}_h$. Again, the linearization algorithm practically works for this extended problem as well, subject to the limitation due to the computing power.

Finally, the design framework described above will be useful for the distributed CPG design for multiple oscillations under various environmental conditions, i.e., the design of a single set of controller parameters σ in (2) to assign different limit cycles (X_k, Λ_k) for different plants (A_k, B_k, C_k) with $k \in \mathbb{I}_h$. In this case, different neuronal dynamics τ_k and oscillation profiles Q_k would facilitate the CPG design and the mapping in (9) would result in different $\mathcal{K}_k(\sigma)$. Thus, the general problem is the simultaneous assignment of multiple eigenstructures by a single controller parameter: Find σ such that $\mathfrak{A}_k(\sigma) := \mathcal{A}_k + \mathcal{B}_k\mathcal{K}_k(\sigma)\mathcal{C}_k$ for $k \in \mathbb{I}_h$ satisfy $\mathfrak{A}_k(\sigma)\mathcal{V}_k = \mathcal{V}_k\Lambda_k$ and the eigenvalues of $\mathfrak{A}_k(\sigma)$ other than those of Λ_k are in the open left half plane. This problem reduces to the simultaneous stabilization of $\mathcal{A}_k(\sigma)$ for $k \in \mathbb{I}_h$ by a structured controller parameter $\sigma \in \mathbb{F}$, and can be formulated as a trace minimization similar to the one described above.

3.4 | CPG Design Procedure

The following summarizes the steps to design an unstructured CPG controller to assign a single gait.

Design Procedure for an Unstructured Controller to achieve a Single Gait for Plant (A, B, C)

1. Specify desired oscillations $x_i(t) = a_i \sin(\omega t + b_i)$ for plant (1) and set (X, Λ) as in (12) with $\hat{x}_i := a_i e^{jb_i}$.
2. Set a controller order n_c and choose a phasor $\hat{q} \in \mathbb{C}^{n_c}$ for a desired oscillation of $q(t)$ so that Q in (12) has full column rank.
3. Choose $\tau > 0$ and set $\alpha := |\hat{q}|$.
4. Solve Problem 2 with Q fixed and find $\mathcal{K}$ through an application of Theorem 1. In particular, solve (15) for U, design $\mathcal{S}(s)$ of order $n_c - 2$ that stabilizes the augmented plant $(A, \mathfrak{B}, C)$, and determine $\mathcal{K}_o$ by (16), or equivalently by (17). Choose a matrix N that makes $T_c := [\, Q \ \ N \,]$ square invertible, and set $\mathcal{K} := T\mathcal{K}_o T^{-1}$ with $T := \mathrm{diag}(I, T_c)$.
5. Solve (9) for $\sigma := (M, G, H, L)$ and the CPG controller is given by (2).

The target oscillation specified in step 1 is achievable if and only if (15) admits a solution U, and the feasibility should be checked before proceeding further. The controller order n_c in step 2 may be chosen as $n_c = n + 2$ so that an observer-based controller of order n can be used for the design of $\mathcal{S}(s)$ in step 4 to stabilize the augmented plant. A model reduction may be performed on such $\mathcal{S}(s)$ to reduce the controller complexity, in which case n_c can be smaller than $n + 2$ (as illustrated by an example later). The amplitude γ for $q(t)$ should be chosen relative to the threshold nonlinearity $\psi(q_i)$. For $\psi(q_i) = \tanh(q_i)$, a

small value (e.g. $\gamma = 0.1$) would make the approximation of ψ by its describing function fairly accurate but a larger value (e.g. $\gamma = 2$) would speed up the convergence to the desired amplitude of oscillation by the nonlinear effect. We suggest to choose the parameter τ in step 3 to reflect the time constant for neuronal processing, which is roughly comparable to (or slightly less than) the cycle period of target body oscillation. The transfer function $\mathcal{S}(s)$ can affect the rate of convergence to the desired phase of oscillation. The parameter N is related to the sensory feedback to the CPG since $H = \tau(QD_{s2} + NB_s)$, and influences how the CPG reacts to perturbations from the target orbit.

The next procedure summarizes the steps to design a structured CPG controller capable of assigning multiple gaits to multiple plants that share the same numbers of actuators and sensors.

Design Procedure for a Structured Controller to achieve h Gaits for Plants (A_k, B_k, C_k) with $k \in \mathbb{I}_h$

1. Specify desired oscillations $x_{k,i}(t) = a_{k,i}\sin(\omega_k t + b_{k,i})$ for plants in (1) with (A, B, C) replaced by (A_k, B_k, C_k), and set (X_k, Λ_k) as in (12) with $\hat{x}_{k,i} := a_{k,i}e^{jb_{k,i}}$ and $k \in \mathbb{I}_h$.
2. Set a controller order n_c and choose $\hat{q}_k \in \mathbb{C}^{n_c}$ for $k \in \mathbb{I}_h$ so that Q_k formed as in (12) has full column rank. For instance, $\hat{q}_k$ with $n_c = m\ell$ can be specified as in (14) from $\hat{x}_k$ by choosing scalars $\gamma_k > 0$ and a common integer $\ell > 0$.
3. Choose $\tau_k > 0$ and set $\alpha_k := |\hat{q}_k|$.
4. Let $(\mathcal{A}_k, \mathcal{B}_k, \mathcal{C}_k)$ and $\mathcal{K}_k(\sigma)$ be defined as in (8) and (9) using the parameters for $k \in \mathbb{I}_h$, and set $\mathfrak{A}_k(\sigma) := \mathcal{A}_k + \mathcal{B}_k\mathcal{K}_k(\sigma)\mathcal{C}_k$, where $\sigma := (M, G, H, L)$. Let $\mathcal{V}_k := \mathrm{col}(X_k, Q_k)$, set $(\mathcal{U}_k, \mathcal{W}_k, \mathcal{N}_k)$ so that the condition corresponding to (18) holds, and define $\mathcal{A}_k(\sigma) := \mathcal{W}_k\mathfrak{A}_k(\sigma)\mathcal{N}_k$.
5. Let $\mathbb{S}$ be a set of matrices with structural constraints that specify the topology of the neural interconnections. With optimization variables P_k, R_k for $k \in \mathbb{I}_h$ and $\sigma \in \mathbb{S}$, minimize the sum of $\mathrm{tr}(P_kR_k)$ over $k \in \mathbb{I}_h$ subject to $\mathcal{A}_k(\sigma)\mathcal{V}_k = \mathcal{V}_k\Lambda_k$ and (22), where P, R, and $\mathcal{A}(\sigma)$ are replaced with P_k, R_k, and $\mathcal{A}_k(\sigma)$ for $k \in \mathbb{I}_h$, and $\varepsilon > 0$ is a small scalar. The CPG controller is given by (2) using the optimal σ.

When multiple oscillations are to be achieved, the CPG would have to be complex enough to embed multiple limit cycles. Increasing the number of neurons in each segment, ℓ, may help in this regard, at the expense of increased computational burden for the design. The neuronal time constants τ_k may be chosen comparable with the cycle periods of target oscillations, and can be useful as a switching parameter for mode transition (see the next section). The cone complementarity linearization algorithm[43] can be used to search for the solution of the optimization problem in step 5. If the optimization turns out to be infeasible, it may help to increase ℓ or relax $\mathbb{S}$ to allow for more neurons and their connections.

4 | DESIGN EXAMPLE: UNDULATORY LOCOMOTION

4.1 | Link-chain Model

We consider a nonlinear robotic system inspired by undulatory locomotion observed in such animals as snakes, eels, and leeches. A dynamical model of such systems with planar motion has been developed in[58,45,46], and is used for our study here. This nonlinear model will be linearized assuming small body curvature with a constant locomotion velocity so that the development in the previous sections can be applied to design a CPG controller. The design will be evaluated by simulating the closed-loop system with the original nonlinear plant model. This section provides a brief summary of the model.

The slender body is represented by a chain of identical n rigid links with flexible joints (Fig. 2, bottom). Each joint is actuated by a torque input and each link is subject to the force from the environment that resists the motion. We consider locomotion along a fixed direction, and take an inertial (x, y) frame so that the x-axis is aligned with the direction of travel. Let $\theta(t) \in \mathbb{R}^n$ be the link angles measured with respect to the x-axis, $u(t) \in \mathbb{R}^{n-1}$ be the joint torque inputs, and $v(t) \in \mathbb{R}$ be the velocity of the center of gravity (CG) of the whole body along the x-axis. With the assumption that link angles θ_i are small and the y component of the CG velocity is negligible, the equations of motion can be expressed in the following form:

$$\begin{aligned} &\mathrm{J}\ddot{\phi} + \mathrm{D}\dot{\phi} + (v\Lambda + \kappa I)\phi = u, \\ &\mathcal{J}\ddot{\varphi} + \mathcal{D}\dot{\varphi} + v^{\mathsf{T}}\phi = 0, \\ &m\dot{v} + d(\phi, \varphi)v + (\dot{\phi}^{\mathsf{T}}\Lambda + \dot{\varphi}^{\mathsf{T}})\phi = 0, \end{aligned} \tag{23}$$

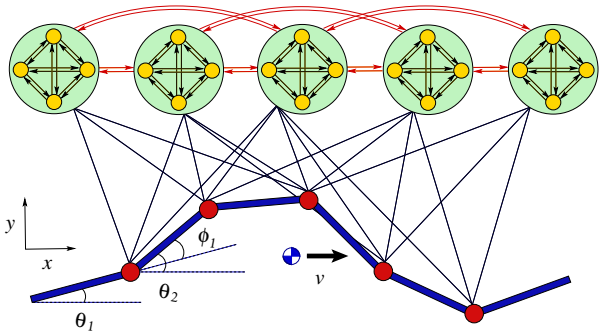

FIGURE 2 Link-Chain System Controlled by Distributed CPG

which are nonlinear, keeping up to the quadratic terms of the variables that are assumed small, where

$$d(\phi, \varphi) := nc_t + nc_o(\varphi - h^\mathsf{T}\phi)^2 + c_o\|T\phi\|^2,$$

and $\phi(t) \in \mathbb{R}^{n-1}$ and $\varphi(t) \in \mathbb{R}$ are the joint angles and body orientation defined by

$$\phi := B^\mathsf{T}\theta, \quad \theta_o := e^\mathsf{T}\theta/n, \quad \varphi := \theta_o + h^\mathsf{T}\phi.$$

Here, the constant coefficient parameters are specified in terms of the joint stiffness κ, the link mass m_o and half length ℓ_o, and tangential and normal drag coefficients c_n and c_t, as follows:

$$\begin{aligned}
&B^\mathsf{T} = \begin{bmatrix} I & o \end{bmatrix} - \begin{bmatrix} o & I \end{bmatrix}, \quad A^\mathsf{T} = \begin{bmatrix} I & o \end{bmatrix} + \begin{bmatrix} o & I \end{bmatrix},\\
&J = m_o l_o^2 (I/3 + F^\mathsf{T}F), \quad T = B(B^\mathsf{T}B)^{-1}, \quad F = TA^\mathsf{T},\\
&\Lambda = c_o l_o F^\mathsf{T}, \quad c_o = c_n - c_t, \quad h = J_{12}J_{22}^{-1},\\
&\begin{bmatrix} J_{11} & J_{12} \\ J_{21} & J_{22} \end{bmatrix} := \begin{bmatrix} T^\mathsf{T} \\ e^\mathsf{T} \end{bmatrix} J \begin{bmatrix} T & e \end{bmatrix},\\
&\mathrm{J} = J_{11} - hJ_{21}, \quad \mathrm{D} = (c_n/m_o)\mathrm{J}, \quad = \Lambda_{21}^\mathsf{T},\\
&\Lambda = \Lambda_{11} - h\Lambda_{21}, \quad \mathcal{D} := (c_n/m_o)\mathcal{J}, \quad \mathcal{J} = J_{22},
\end{aligned}$$

where $o \in \mathbb{R}^{n-1}$ and $e \in \mathbb{R}^n$ are vectors with all entries equal to zero and one, respectively, and Λ_{ij} are defined in a manner similar to J_{ij} for $i, j = 1, 2$.

For the parameter values of the link-chain model, we use the typical properties of a leech[46] with length $\ell = 10$ cm, width $d = 1$ cm, and weight $m = 1$ g. Since each link is assumed to be identical, each individual link has half length $l_o = l/(2n)$ and mass $m_o = m/n$, where we assume $n = 6$ links. The stiffness for each joint is set to $\kappa = 4.26$ (mN·cm)/rad, which was chosen such that the flexible body would have a natural frequency at 3 Hz as roughly observed in leeches[15]. We consider two different fluid environments for leech swimming: water and methyl cellulose, where the latter has viscosity 400 times higher than the former. Using a simple model of hydrodynamic forces in[46], the fluid drag coefficients are given by $(c_n, c_t) = (8.08, 0.47)$ in water and $(c_n, c_t) = (1.56, 1.17)$ in methyl cellulose.

4.2 | Target Oscillations and Control Framework

The leech swims by undulating its body, sending traveling waves from head to tail. The body shape change, or the gait, is specified by the frequency ω, amplitudes a_i, and phases b_i of the joint angles $\phi_i(t) \cong a_i \sin(\omega t + b_i)$ for $i = 1, \ldots, 5$. We set the desired oscillation profile for the control design based on observational data from real leeches swimming in water and methyl cellulose[15]. A typical gait in water is given in Table 1, where the amplitude increases and the phase decreases toward tail (link 1 is tail and link 6 is head). Also indicated are the amplitudes and phases of the control input $u(t)$ that generates the given target gait $\phi(t)$. The phasor $\hat{u}$ is estimated from (23) as

$$\hat{u} = (-\omega^2\mathrm{J} + j\omega\mathrm{D} + v_o\Lambda + \kappa I)\hat{\phi}, \quad \hat{\phi}_i := a_i e^{jb_i},$$

where v_o is the average of the swim speed $v(t)$ resulting from the gait $\phi(t)$. Table 2 shows the data for a typical gait in methyl cellulose, where the phase shift between joints is larger, indicating a smaller wavelength of the body curvature waves. With the

slightly reduced undulation frequency, the resulting swim speed is much smaller than that in water due to the increased viscous drag.

TABLE 1 Target Oscillation Profile in Water

	ϕ_1	ϕ_2	ϕ_3	ϕ_4	ϕ_5
Amplitude [deg]	34.00	32.75	31.50	30.25	29.00
Phase [deg]	0	60.0	120.0	180.0	240.0

	u_1	u_2	u_3	u_4	u_5
Amplitude [mN·cm]	190	75	233	324	280
Phase [deg]	-10.0	100.2	183.4	215.2	248.4

Frequency: $\omega = 3$ Hz, Swim Speed: $v_o = 15.6$ cm/s

TABLE 2 Target Oscillation Profile in Methyl Cellulose

	ϕ_1	ϕ_2	ϕ_3	ϕ_4	ϕ_5
Amplitude [deg]	34.00	32.75	31.50	30.25	29.00
Phase [deg]	0	90.0	180.0	270.0	360.0

	u_1	u_2	u_3	u_4	u_5
Amplitude [mN·cm]	249	222	215	228	222
Phase [deg]	-1.7	89.0	185.0	274.9	360.9

Frequency: $\omega = 2$ Hz, Swim Speed: $v_o = 0.24$ cm/s

We will design controllers for the leech model to achieve one or both of the target oscillations. The overall closed-loop system is depicted in Fig. 3, where the local and global motion blocks represent the equations of motion for ϕ and (φ, v) in (23), respectively, and the CPG block represents the dynamics in (2) with sensory input of joint angles, $y := \phi$, which may correspond to proprioceptive feedback of muscle strain. When the body shape $\phi(t)$ changes periodically, the locomotion velocity $v(t)$ will oscillate with a nonzero average value, v_o, in general. The controller will be designed using the local motion model (i.e. the first equation in (23)) with a constant velocity $v(t) \equiv v_o$, which defines the linear time-invariant plant in (1) with state $x := \mathrm{col}(\phi, \dot{\phi})$. The phasor $\hat{\phi}$ and frequency ω specified in each of Tables 1 and 2 define the target eigenstructure for the plant (X, Λ) as in (12) with $\hat{x} := \mathrm{col}(\hat{\phi}, j\omega\hat{\phi})$. The methods for eigenstructure assignment described in the previous section are then applied to obtain controllers. We will first design a centralized controller to achieve the nominal gait in Table 1, and then design a distributed controller, of the structure shown in Fig. 2, that achieves either of the two gaits in Tables 1 and 2, depending on the value of the time constant τ. Finally, an adaptation mechanism for τ will be added to the latter controller to allow for autonomous gait transition in accordance with the changing environment, in which case, there will be an additional exteroceptive sensory feedback of the locomotion speed v to the CPG block in Fig. 3. The designs will be evaluated by simulating the closed-loop system with the entire nonlinear dynamics in (23) for the plant.

4.3 | Centralized CPG for Nominal Gait in Water

In our first example, we utilize the Design Procedure for an Unstructured Controller described in Section 3.4 to obtain a feasible controller that assigns the gait for the leech in water. More specifically, we design a feedback controller (2) such that the profiles of the closed-loop oscillations for $\phi(t)$ and $u(t)$ are approximately given by the phasors $\hat{\phi}$ and $\hat{u}$ in Table 1. We define the dynamics of each neuron by a low-pass filter with time constant $\tau = 0.2$ s, which is typical for neuronal processes. We choose the total number of controller states equal to the number of actuators, i.e., $q(t) \in \mathbb{R}^5$. The target phasor for the controller state $q(t)$ is set to have uniform amplitude $\gamma = 1$ and phases aligned with the target input $u(t)$, that is, $\hat{q}_i = \gamma e^{j\angle\hat{u}_i}$, which is a special case of (14) with $\ell = 1$.

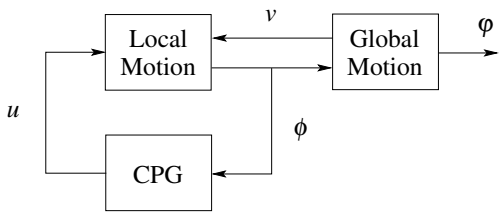

FIGURE 3 Locomotion System with CPG Control

The controller is designed as follows. First, the desired eigenstructure (X, Q, Λ) is set as in (12) with $\hat{x} := \mathrm{col}(\hat{\phi}, j\omega\hat{\phi})$. Second, an observer-based stabilizing controller $\mathcal{S}(s)$ in (16) is designed for the augmented plant $(A, \mathfrak{B}, C)$. The stabilizing controller $\mathcal{S}(s)$ is chosen to be the LQG controller with all the weights in the cost function and noise covariances equal to identity matrices. The resulting controller $\mathcal{S}(s)$ turned out to be a stable 10^{th} order system, and was transformed into the balanced realization and then truncated to retain 3 states only so that the overall linear controller $\mathcal{K}_o$ in (17) has 5 states due to the addition of the internal model dynamics involving Λ. A state coordinate transformation $q = T_c q_o$ is then performed on the state $q_o := \mathrm{col}(\zeta, x_s)$ of $\mathcal{K}_o$ so that the target phasor $\hat{q}$ is achieved for the state q of the resulting controller $\mathcal{K}$. The similarity transformation matrix is $T_c = [Q\ \varrho N]$, where N is chosen so that its columns form an orthonormal basis for the null space of Q^{T}, and $\varrho = 100$. Finally, the CPG parameters are found by solving (9) for (M, H, G, L) where $\alpha \in \mathbb{R}^5$ is the vector with all entries equal to $\gamma = 1$.

The closed-loop system of (23) and (2) is simulated to evaluate the control design. The initial condition is set so that the slender body is straight at rest and aligned with the x-axis ($\phi(0) = \dot{\phi}(0) = 0$ and $\varphi(0) = v(0) = 0$), and the CPG states are all equal to one ($q(0) = \mathrm{col}(1, \dots, 1)$). The result for the first 3 seconds is plotted in Fig. 4. The oscillations converge within several cycles and the velocity eventually converges to an average value of 14.7 cm/s. Although the controller design was performed using a simplified linear time-invariant model that assumed a constant velocity $v(t) \equiv v_o$, the nonlinear simulation which included the entire nonlinear dynamics in (23) saw approximate entrainment to the desired velocity.

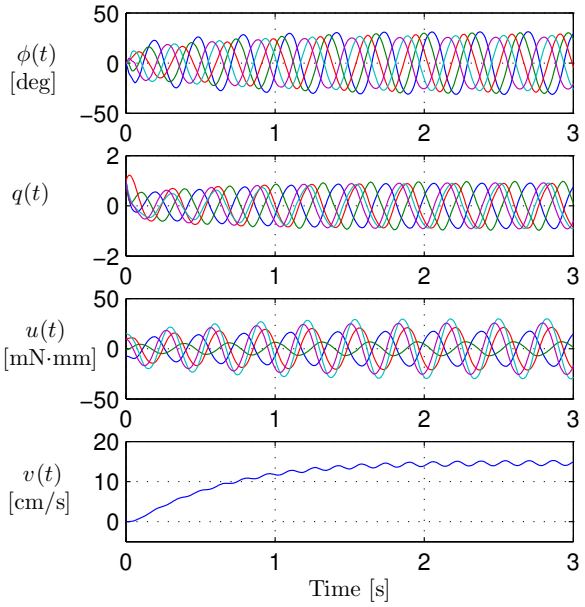

FIGURE 4 Closed-Loop Simulation in Water Environment

The amplitudes, phases, and frequency of the first harmonic component of the oscillation profile obtained through Fourier analysis are tabulated in Table 3. We see that the simulated steady state behavior of body shape $\phi(t)$ is fairly close to the desired values in Table 1 for each specification. The phases of the CPG states $q(t)$ are roughly aligned with those of the control input $u(t)$

as designed. Thus we conclude that the proposed CPG design method based on Theorem 1 is effective in achieving the desired gait for the undulatory locomotion system.

TABLE 3 Oscillation Profile in Water with Controller (16)

	ϕ_1	ϕ_2	ϕ_3	ϕ_4	ϕ_5
Amplitude [deg]	32.13	30.29	28.43	27.50	26.86
Phase [deg]	0	58.3	119.3	180.7	241.3

	q_1	q_2	q_3	q_4	q_5
Amplitude	0.91	0.92	0.89	0.88	0.92
Phase [deg]	-10.4	101.0	187.1	214.3	249.5

	u_1	u_2	u_3	u_4	u_5
Amplitude [mN·cm]	176	70	216	302	261
Phase [deg]	-8.8	101.3	184.7	216.6	249.7

Frequency: $\omega = 3.12$ Hz, Swim Speed: $v_o = 14.7$ cm/s

4.4 | Distributed CPG for Adaptive Gaits

For this design example, we apply the Design Procedure for a Structured Controller described in Section 3.4 to obtain a feasible controller to assign the oscillation profiles for the link-chain model in both water and the methyl cellulose as specified in Tables 1 and 2. If we interpret each assigned eigenstructure as a different gait for a mechanical system and different plants as variations in the environment, then the design of a single controller that can achieve different limit cycles for different plants would imply an adaptation property embedded in the controller.

In the design, we constrain the controller to have a distributed architecture as shown in Fig. 2. A segmental oscillator (green circle) consisting of four neurons (yellow circles) is placed for each joint, directly communicating with its immediate and second neighbors (red arrows). The chain of oscillators, with 20 neurons all together, forms a CPG with state vector $q(t) \in \mathbb{R}^{20}$. Each segmental oscillator collects sensing information (ϕ_i) from, and sends actuation signals (u_i) to, its neighboring joints (black lines). The controller is thus described by (2) with the added condition that the matrix parameters (L, G, H, M) all have a block penta-diagonal structure. For example, the neuronal connectivity matrix, M, is constrained to have the following structure,

$$M = \begin{bmatrix} M_{11} & M_{12} & M_{13} & 0 & 0 \\ M_{21} & M_{22} & M_{23} & M_{24} & 0 \\ M_{31} & M_{32} & M_{33} & M_{34} & M_{35} \\ 0 & M_{42} & M_{43} & M_{44} & M_{45} \\ 0 & 0 & M_{53} & M_{54} & M_{55} \end{bmatrix},$$

where M_{ii} specifies the interconnections of the neurons within one segmental oscillator and M_{ij} for $i \neq j$ specifies the interconnection between the segmental oscillators; the structures of L, G, and H are defined similarly, except that $L_{ij} \in \mathbb{R}$, $G_{ij} \in \mathbb{R}^{1\times 4}$, and $H_{ij} \in \mathbb{R}^{4\times 1}$, while $M_{ij} \in \mathbb{R}^{4\times 4}$. This defines the structured set $\mathbb{S}$ introduced in Section 3.3.

The target phasor for the controller state $\hat{q} \in \mathbb{C}^{20}$ is specified as described in (14), where the number of segmental oscillators is $m = 5$, and the number of neurons within each segment is $\ell = 4$. The phases within each segmental oscillator are equally spaced over 2π, while the intersegmental phase shifts are aligned with the control input $u(t) \in \mathbb{R}^5$. For the two gaits in water and methyl cellulose, two target phasors $\hat{q}$ are obtained using the $\hat{u}$ described in Tables 1 and 2. The oscillation amplitude for the target $q(t)$ is set to $\gamma = 1.5$ for both cases in order to obtain a fair approximation of the desired oscillation while remaining in the nonlinear zone of the describing function.

The two sets of eigenstructures $\mathcal{V}_k := (X_k, Q_k)$ and Λ_k are thus specified for the target gaits in water ($k = 1$) and methyl cellulose ($k = 2$). Since the undulation frequencies of the target gaits are different, we will set different time constants τ for the CPG controller, allowing for gait transition by simply switching the value of τ in accordance with the given fluid environment. Specifically, we use $\tau = 0.2$ s in water and $\tau = 0.3$ s in methyl cellulose. The different τ values give different mapping $\mathcal{K}_k(\sigma)$ in (9). The closed-loop matrices $\mathfrak{A}_k(\sigma)$ for $k = 1, 2$ are defined as in (7), together with the plant models (A_k, B_k, C_k) obtained from

the first equation in (23) with the two sets of values for (c_n, c_t) and $v(t) \equiv v_o$. A controller is then designed by numerically solving the trace optimization as described in Section 3.3. In the example that follows, we perform the controller search with $\varepsilon = 0.01$.

4.4.1 | Steady-State Oscillation Profiles

To first test whether the designed controller achieves convergence to each of the target oscillation profiles, we simulate the nonlinear closed-loop system of (23) and (2) to start from initial conditions with zero plant states $(\phi, \dot{\phi}, \varphi, \dot{\varphi}, v)$ and random controller states q. Simulations are run in water and methyl cellulose environments, where the plant and controller model parameters are identical for both cases except that the values of (c_n, c_t, τ) are $(8.08, 0.47, 0.2)$ in water and $(1.56, 1.17, 0.3)$ in methyl cellulose.

Figure 5 (top) gives the steady state oscillations of the joint angles $\phi_i(t)$ in a water environment. The amplitudes, phases, and frequency of the first harmonic component of $\phi(t)$ obtained through Fourier analysis are shown below in Table 4. While the oscillation profile does not match exactly with respect to amplitude, the frequency of oscillation and phases match very closely to the desired profile. Even in the case of amplitude, all the amplitudes are within 20% of desired and share a similar pattern of increasing amplitudes from head to tail. Also shown in Fig. 5 are some of the controller states $q_i(t)$. The amplitudes are roughly uniform with magnitude approximately equal to $\gamma = 1.5$ as designed. The middle plot indicates the controller states for the first neuron of every segmental oscillator. The phase shifts between segments are close to those of $\hat{u}$ in Table 1. The bottom plot shows the controller states within the first segmental oscillator, where the phases are equally spaced over 2π, confirming effectiveness of the design method. The nominal velocity obtained through simulation is lower than the desired nominal velocity of 15.6 cm/s by roughly 10% at 13.93 cm/s. Thus, the controller designed roughly approximates the desired specifications for the link-chain system in water.

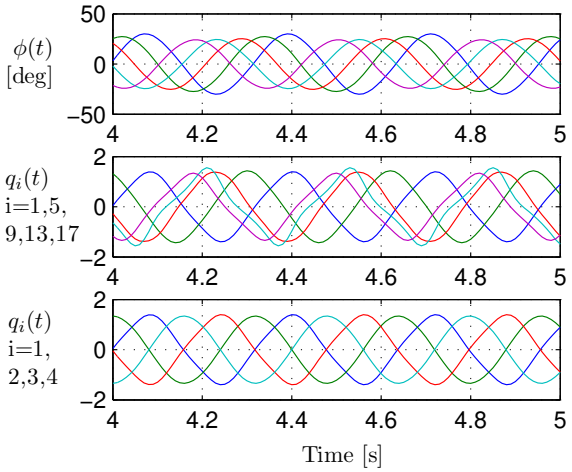

FIGURE 5 Simulated $\phi(t)$ and $q(t)$ in Water Environment

TABLE 4 Oscillation Profile inside Water Environment using Multi-gait Structured Controller

	ϕ_1	ϕ_2	ϕ_3	ϕ_4	ϕ_5
Amplitude [deg]	29.67	27.85	25.46	24.29	24.49
Phase [deg]	0	59.56	118.4	179.0	235.3

Frequency: $\omega = 3.13$ Hz, Swim Speed: $v_o = 13.9$ cm/s

The same controller with the adjusted τ value functions even better in meeting the specification for the case where the link-chain system is placed in methyl cellulose as evidenced in Fig.6. With the change in the plant to replicate a different fluid environment, the oscillation profile changes to match the one prescribed for methyl cellulose. Table 5 gives specific numbers

regarding the simulated oscillation profile of the link-chain model in the high-viscosity environment. A comparison with Table 2 reveals that the controller achieves the prescribed oscillation better in methyl cellulose than in water. Every amplitude is within 5% of the desired value with the phases and frequency of oscillation following a similar trend. Because the oscillation profile of the nonlinear simulation so closely matches that of the designed profile, the simulated velocity also closely matches that of the desired, deviating by under 10% at 0.223 cm/s.

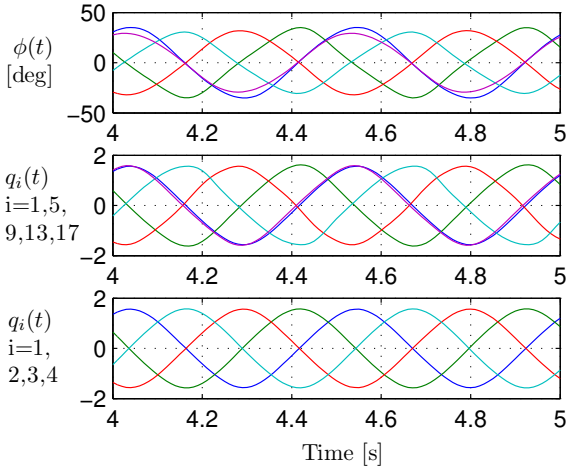

FIGURE 6 Simulated $\phi(t)$ and $q(t)$ in High-Viscosity Environment

TABLE 5 Oscillation Profile inside Methyl Cellulose using Multi-gait Structured Controller

	ϕ_1	ϕ_2	ϕ_3	ϕ_4	ϕ_5
Amplitude [deg]	34.67	32.63	31.34	29.07	29.24
Phase [deg]	0	92.76	180.3	276.2	362.9

Frequency: $\omega = 1.97$ Hz, Swim Speed: $v_o = 0.223$ cm/s

Snapshots for the body shape of each of these gaits over one period is given in Fig. 7, where the time elapses from top to bottom. The horizontal shift of the body location indicates progression due to swimming to the right, which is visible in water but invisibly small in methyl cellulose due to high viscosity. The wavelength of the body undulation is roughly equal to the body length in water, but it is reduced in the high viscosity fluid. It should be noted that these snapshots of the closed-loop link-chain model, obtained through designing a single structured controller to assign two different gaits, very closely match the observed gaits of biological leeches in water and methyl cellulose [15], the data of which is used to set the target gaits.

In biology, the neuronal CPG circuits are nonlinear oscillators by themselves when isolated from the body dynamics, exhibiting patterned oscillations resembling observed kinematics [15]. In our control design, we specified the oscillation profile of the closed-loop system, but did not explicitly require the controller (i.e. CPG) by itself to be an oscillator. However, when the designed CPG controller with $\tau = 0.2$ s is simulated without sensory feedback ($H = 0$, $L = 0$) with a nonzero initial state, the state $q(t)$ was found to converge to a stable limit cycle, and the resulting control input $u(t)$ oscillates as shown in Fig. 8. Thus, the controller alone is an oscillator with a specific phase/amplitude property, justifying that it can indeed be called a CPG. The oscillation profile of $u(t)$ is similar to but different from that of the closed-loop simulation. In particular, the phase lag from head (purple) to tail (blue) is much larger with sensory feedback (note the spread of the peak locations), which is consistent with observations from the intact and isolated nerve cords of leeches [59,47,15]. Thus, the proposed design method yielded the biological control architecture of a nonlinear oscillator (CPG) placed in a feedback loop, with some similarity in the phase property. We also found that, if the open-loop CPG control is applied, the resulting body undulation becomes almost standing waves in both

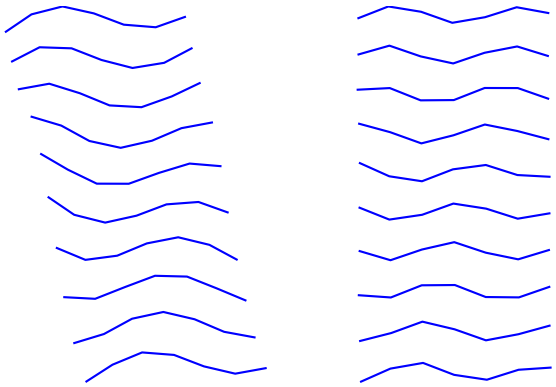

FIGURE 7 Snapshots of One Cycle of the Simulated Leech Gait in Water (left) and Methyl Cellulose (right)

water and methyl cellulose, with much larger body curvature in the latter fluid. Thus, the gait can change due to the environmental factor alone, but the particular gaits observed in biology appear to be a result of intricate *mutual* entrainment of the CPG and the surrounding physical dynamics where sensory feedback plays a crucial role. However, details of the neural control (e.g. the number of neurons, network topology, synaptic weights, afferent signals) are not captured by our controller, and biological implications of our design method need more careful investigation.

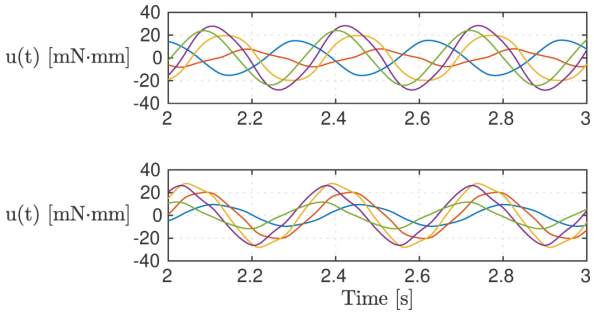

FIGURE 8 CPG Control Input $u(t)$ with (top) and without (bottom) Sensory Feedback

4.4.2 | Gait Transition

The previous section showed that the structured controller entrains to both designed oscillation profiles in the steady state. This section tests whether the CPG-based controller exhibits adaptive behaviors similar to that observed in biological CPGs, namely, the ability to change gaits when exposed to different environments. To enable autonomous gait transition, we need an adaptation mechanism to adjust the time constant τ in the CPG controller in accordance with the environment. Such mechanism may be implemented in various ways depending on the available sensing information. While full exploration of possible options is out of the scope of this paper, here we assume availability of a swim velocity measurement. The time constant τ in the CPG controller is adjusted in real time by

$$\tau = 0.25 - 0.05 \tanh(v - 3).$$

This mechanism allows for autonomous transition of τ between 0.2 s at high speed and 0.3 s at low speed where the threshold velocity is $v = 3$ cm/s. The idea is to use the nominal gait (Fig.7, left) when swimming near the nominal velocity $v = 13.9$ cm/s, and transition to the other gait (Fig.7, right) when the nominal gait results in a swim speed lower than the threshold due to the change of the environment. The steady state speed achieved by the controller with $\tau = 0.3$ in water is about $v = 5.7$ cm/s, and the speed with $\tau = 0.2$ in methyl cellulose is about $v = 1.0$ cm/s. The threshold $v = 3$ cm/s is chosen to be a value in the interval $1.0 < v < 5.7$.

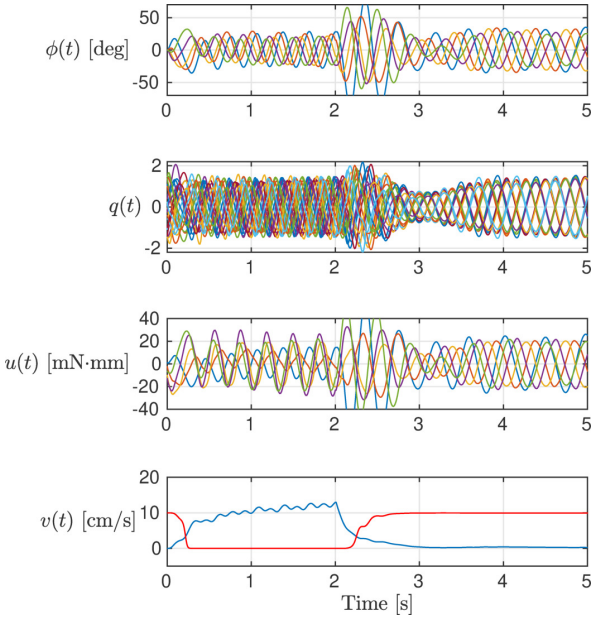

FIGURE 9 Closed-Loop Simulation for Gait Switching

We simulated the controller with the τ adaptation mechanism applied to the link-chain system in water and then, after the profile reached near the steady-state orbit we switched the plant model to the one representing the link-chain system in methyl cellulose to emulate a change in environment. The results of this simulation are given in Fig. 9, where the switching of the environment occurs at $t = 2$ s. The automatic adaptation of τ is also indicated by the red curve in the bottom plot where $100(\tau - 0.2)$ is shown to fit the curve on the same scale. Starting with $v = 0$ in water, the controller with $\tau \cong 0.3$ accelerates the body to go beyond the velocity threshold and smoothly transitions to the mode with $\tau \cong 0.2$, resulting in the nominal gait in water. When the body enters the high viscosity environment at $t = 2$, it decelerates down below the velocity threshold due to the large drag. As a result, the controller transitions back to the mode with $\tau \cong 0.3$, and the oscillation converges to the target gait in methyl cellulose within several cycles. If the adaptation mechanism is removed and the controller is fixed with time constant $\tau = 0.2$, then the swimming body struggles with a large undulation ($\max \phi_i(t) \cong 55^o$) using a large control input ($\max u_i(t) \cong 39$ mN·mm) in the steady state. Thus, the autonomous gait transition is effective for keeping the control effort at a reasonable level.

From this example, it is clear that the proposed eigenstructure assignment method can be applied, with an additional parameter adaptation mechanism, to the design of a single distributed controller that can change gaits depending on the plant. Moreover, since a variation in the plant can represent a change in the environment, the design capability allows for the controller to autonomously change gaits depending on variations in environments. Although the proposed design method for multi-gait eigenstructure assignment relies on the trace minimization for which global convergence is not guaranteed, the example provided above shows that the problem is certainly feasible and the method can be practically useful.

5 | CONCLUSION

In this paper, we considered the design of a controller to replicate the functionality of the central pattern generator, a collection of neurons responsible for animal locomotion. This problem was formulated as the design of a nonlinear controller for a linear plant to assign a stable limit cycle to the closed-loop system. This was approximately reduced to the search for a linear controller to assign a pair of eigenvalues and corresponding eigenvectors to achieve coordinated oscillations. We have shown how an eigenstructure assignment theory from the literature can be applied to the design of feedback controllers with the CPG architecture. An example was given to demonstrate the efficacy of the proposed method by designing a CPG-based controller for a link-chain model in order to replicate the observed gait of biological leeches in water.

The method for designing a CPG-based controller was further expanded to encompass the assignment of multiple gaits by a single controller of a prescribed distributed structure, to cope with varying dynamics in the environment. This problem was

reduced, essentially, to the search of a single structured controller to simultaneously assign multiple eigenstructures for multiple plants. We provided an example in which a single structured CPG-based controller was designed to assign the observed gaits of biological leeches in water and high-viscosity fluid (methyl cellulose). The simultaneous eigenstructure assignment with an additional adjustment of the neural time constant yielded a closed-loop system that exhibited adaptive behavior similar to that observed in biological CPGs. Specifically, numerical simulations confirmed that the CPG-based controller was capable of switching between the two designed gaits when the plant was changed to reflect a change between the two fluids.

While we demonstrated that eigenstructure assignment can be used for effective design of CPG-based controllers, more research must be performed to expand on this result. In particular, we do not provide a rigorous theoretical guarantee for existence and stability of the limit cycles in the closed-loop system. The method of harmonic balance is approximate and could fail to produce stable oscillations. Furthermore, the proposed method for multi-eigenstructure assignment is based on a numerical optimization, which is computationally demanding and may not be practical for high-complexity problems with large numbers of neurons, plant state variables, and target limit cycles. Future research efforts should address these issues.

References

1. Ijspeert A. Central pattern generators for locomotion control in animals and robots: A review. *Neural Networks* 2008; 21: 642-653.
2. Yu J, Tan M, Chen J, Zhang J. A survey on CPG-inspired control models and system implementation. *IEEE Transactions on Neural Networks and Learning Systems* 2014; 25(3): 441-456.
3. Delcomyn F. Neural Basis of Rhythmic Behavior in Animals. *Science* 1980; 210(4469): 492–498.
4. Grillner S, Ekeberg Ö, El Manira A, et al. Intrinsic function of a neuronal network - a vertebrate central pattern generator. *Brain Research Reviews* 1998; 26(2): 184–197.
5. Jean A. Brainstem control of swallowing: localization and organization of the central pattern generator for swallowing. In: Springer. 1990 (pp. 294–321).
6. Marder E, Bucher D. Central pattern generators and the control of rhythmic movements. *Current Biology* 2001; 11(23): R986–R996.
7. Guertin PA. The mammalian central pattern generator for locomotion. *Brain Research Reviews* 2009; 62(1): 45–56.
8. Duysens J, Crommert V. dHW. Neural control of locomotion; Part 1: The central pattern generator from cats to humans. *Gait & posture* 1998; 7(2): 131–141.
9. Jr. WK, Calabrese R, Friesen W. Neuronal control of leech behavior. *Prog. in Neurobiol.* 2005; 76: 279-327.
10. Friesen W, Poon M, Stent G. Neuronal control of swimming in the medicinal leech IV. Identification of a network of oscillatory interneurones. *J. Exp. Biol.* 1978; 75: 25-43.
11. Cohen AH, Wallén P. The Neuronal Correlate of Locomotion in Fish. *Experimental Brain Research* 1980; 41(1): 11–18.
12. Eisenhart FJ, Cacciatore TW, Kristan Jr WB. A central pattern generator underlies crawling in the medicinal leech. *Journal of Comparative Physiology A* 2000; 186(7-8): 631–643.
13. Zhong G, Shevtsova NA, Rybak IA, Harris-Warrick RM. Neuronal activity in the isolated mouse spinal cord during spontaneous deletions in fictive locomotion: insights into locomotor central pattern generator organization. *The Journal of Physiology* 2012; 590(19): 4735–4759.
14. Bucher D, Haspel G, Golowasch J, Nadim F. Central pattern generators. *eLS. John Wiley & Sons, Ltd. DOI: 10.1002/9780470015902.a0000032.pub2* 2015.
15. Iwasaki T, Chen J, Friesen W. Biological clockwork underlying adaptive rhythmic movements. *Proc. National Academy of Sciences of USA* 2014; 111(3): 978-983.

16. Yu X, Nguyen B, Friesen WO. Sensory feedback can coordinate the swimming activity of the leech. *J. Neurosci.* 1999; 19(11): 4634-4643.

17. Taga G. Self-organized control of bipedal locomotion by neural oscillators in unpredictable environment. *Biol. Cybern.* 1991; 65(3): 147-159.

18. Buchli J, Ijspeert A. Distributed central pattern generator model for robotics application based on phase sensitivity analysis. *BioADIT* 2004; 3141: 333–349.

19. Lodi M, Shilnikov A, Storace M. Design of Synthetic Central Pattern Generators Producing Desired Quadruped Gaits. *IEEE Transactions on Circuits and Systems* 2018; 65(3): 1028-1039.

20. Lodi M, Shilnikov A, Storace M. Design Principles for Central Pattern Generators With Preset Rhythms. *IEEE Transactions on Neural Networks and Learning Systems* 2019; DOI: 10.1109/TNNLS.2019.2945637.

21. Arena P, Fortuna L, Frasca M. Multi-template approach to realize central pattern generators for artificial locomotion control. *Int. J. Circuit Theory and Applications* 2002; 30: 441-458.

22. Ijspeert A. A connectionist central pattern generator for the aquatic and terrestrial gaits of a simulated salamander. *Biol. Cybern.* 2001; 84: 331-348.

23. Ijspeert A, Crespi A, Ryczko D, Cabelguen J. From swimming to walking with a salamander robot driven by a spinal cord model. *Science* 2007; 315(5817): 1416-1420.

24. Brown T. The intrinsic factors in the act of progression in the mammal. *Proc. Roy. Soc. Lond.* 1911; 84: 308-319.

25. Golubitsky M, Stewart I, Buono PL, Collins JJ. Symmetry in locomotor central pattern generators and animal gaits. *Nature* 1999; 401(6754): 693-695.

26. Pinto CMA, Golubitsky M. Central pattern generators for bipedal locomotion. *Journal of Mathematical Biology* 2006; 53(3): 474-489.

27. Danner SM, Wilshin SD, Shevtsova NA, Rybak IA. Central control of interlimb coordination and speed-dependent gait expression in quadrupeds. *The Journal of Physiology* 2016; 594(23): 6947-6967.

28. Pogromsky A, Santoboni G, Nijmeijer H. Partial synchronization: from symmetry towards stability. *Physica D* 2002; 172: 65-87.

29. Pham Q, Slotine J. Stable concurrent synchronization in dynamic system networks. *Neural Networks* 2007; 20: 62-77.

30. Liu X, Iwasaki T. Design of coupled harmonic oscillators for synchronization and coordination. *IEEE Trans. Auto. Contr.* 2017; 62(8): 3877-3889.

31. Kimura H, Akiyama S, Sakurama K. Realization of dynamic walking and running of the quadruped using neural oscillator. *Autonomous Robots* 1999; 7(3): 247-258.

32. Futakata Y, Iwasaki T. Formal analysis of resonance entrainment by central pattern generator. *J. Math. Biol.* 2008; 57(2): 183-207.

33. Futakata Y, Iwasaki T. Entrainment to natural oscillations via uncoupled central pattern generators. *IEEE Trans. Auto. Contr.* 2011; 56(5): 1075-1089.

34. Buchli J, Iida F, Ijspeert A. Finding resonance: Adaptive frequency oscillators for dynamic legged locomotion. In: ; 2006: 3903-3909.

35. Righetti L, Ijspeert A. Programmable central pattern generators: an application to biped locomotion control. *IEEE Int. Conf. Robotics and Automation* 2006: 1585-1590.

36. Zhao J, Iwasaki T. Orbital stability analysis for perturbed nonlinear systems and natural entrainment via adaptive Andronov-Hopf oscillator. *IEEE Trans. Auto. Contr.* 2020; 65(1): 87-101.

37. Chung S, Dorothy M. Neurobiologically inspired control of engineered flapping flight. *J. Guid. Contr. Dyn.* 2010; 33(2): 440-453.

38. Seo K, Chung S, Slotine J. CPG-based control of a turtle-like underwater vehicle. *Auton. Robot* 2010; 28(3): 247-269.

39. Chen Z, Iwasaki T. Circulant synthesis of central pattern generators with application to control of rectifier systems. *IEEE Trans. Auto. Contr.* 2008; 53(3): 273-286.

40. Iwasaki T. Multivariable harmonic balance for central pattern generators. *Automatica* 2008; 44(12): 4061-4069. (DOI:10.1016/j.automatica.2008.05.024).

41. Wu A, Iwasaki T. Pattern Formation Via Eigenstructure Assignment: General Theory and Multi-Agent Application. *IEEE Transactions on Automatic Control* 2018; 63(7): 1959-1972.

42. Grigoriadis K, Skelton R. Low-order control design for LMI problems using alternating projection methods. *Automatica* 1996; 32: 1117-1125.

43. Ghaoui LE, Oustry F, AitRami M. A cone complementarity linearization algorithm for static output-feedback and related problems. *IEEE Trans. Auto. Contr.* 1997; 42(8): 1171-1176.

44. Orsi R, Helmke U, Moore J. A Newton-like method for solving rank constrained linear matrix inequlaities. *Automatica* 2006; 42: 1875-1882.

45. Blair J, Iwasaki T. Optimal gaits for mechanical rectifier systems. *IEEE Trans. Auto. Contr.* 2011; 56(1): 59-71.

46. Chen J, Friesen W, Iwasaki T. Mechanisms underlying rhythmic locomotion: Body-fluid interaction in undulatory swimming. *J. Exp. Biol.* 2011; 214(4): 561-574.

47. Zheng M, Friesen W, Iwasaki T. Systems-level modeling of neuronal circuits for leech swimming. *J. Computational Neuroscience* 2007; 22(1): 21-38.

48. Iwasaki T, Wen M. Control design for coordinated oscillations with central pattern generator. *Proc. American Control Conference* 2013: 2972-2977.

49. Wu A, Iwasaki T. Feedback control for oscillations with CPG architecture. *Proc. IEEE Conf. Dec. Contr.* 2014.

50. Khalil H. *Nonlinear Systems*. Prentice Hall . 1996.

51. Cohen A, Rossignol S, Grillner S. *Neural Control of Rhythmic Movements in Vertebrates*. Wiley-Interscience . 1988.

52. Grillner S, Buchanan J, Walker P, Brodin L. *Neural Control of Rhythmic Movements in Vertebrates*. New York: Wiley . 1988.

53. Koch C, Segev I. *Methods in Neuronal Modeling: From Synapses to Networks*. The MIT Press . 1989.

54. Orlovsky G, Deliagina T, Grillner S. *Neuronal Control of Locomotion: From Mollusc to Man*. Oxford University Press . 1999.

55. Friesen W, Friesen J. *NeuroDynamix: Computer models for neurophysiology*. Oxford University Press . 1994.

56. Williams T. Phase coupling by synaptic spread in chains of coupled neuronal oscillators. *Science* 1992; 258(5082): 662-665.

57. Iwasaki T, Hara S. Generalized KYP lemma: Unified frequency domain inequalities with design applications. *IEEE Trans. Auto. Contr.* 2005; 50(1): 41-59.

58. Saito M, Fukaya M, Iwasaki T. Serpentine locomotion with robotic snake. *IEEE Control Systems Magazine* 2002; 22(1): 64-81.

59. Pearce R, Friesen W. Intersegmental coordination of leech swimming: comparison of in situ and isolated nerve cord activity with body wall movement. *Brain Res.* 1984; 299: 363-366.